RSC Advances

This is an *Accepted Manuscript*, which has been through the Royal Society of Chemistry peer review process and has been accepted for publication.

Accepted Manuscripts are published online shortly after acceptance, before technical editing, formatting and proof reading. Using this free service, authors can make their results available to the community, in citable form, before we publish the edited article. This *Accepted Manuscript* will be replaced by the edited, formatted and paginated article as soon as this is available.

You can find more information about *Accepted Manuscripts* in the Information for Authors.

Please note that technical editing may introduce minor changes to the text and/or graphics, which may alter content. The journal's standard Terms & Conditions and the Ethical guidelines still apply. In no event shall the Royal Society of Chemistry be held responsible for any errors or omissions in this *Accepted Manuscript* or any consequences arising from the use of any information it contains.

ROYAL SOCIETY OF CHEMISTRY

www.rsc.org/advances

RSC Advances

RSCPublishing

ARTICLE

Impact of chain morphology on the lubricity of surface-grafted polysaccharides

Cite this: DOI: 10.1039/x0xx00000x

T. Goren,[a] N. D. Spencer[a] and R. Crockett[b,*],

Received 00th January 2012,
Accepted 00th January 2012

DOI: 10.1039/x0xx00000x

www.rsc.org/

Surface-density gradients of dextran have been fabricated on silicon wafers by means of an intermediate azide-terminated monolayer, which binds to random segments of the dextran chains to form a complex loop-train-tail structure. Friction-force microscopy was employed to understand the relative contributions of chain density and other parameters on the tribological behaviour of the immobilized chains. The results are contrasted with similar investigations performed with density gradients of poly(L-lysine)-*graft*-dextran, a bottlebrush copolymer that adsorbs onto silica to form a well-characterized dextran brush. Both systems exhibit friction coefficients that vary over more than an order of magnitude with applied load, with a sharp transition from low- to high-friction regimes occurring upon increasing load. The brush architecture exhibited more extreme friction coefficients than the loop-train-tail architecture, lubricating better at low loads while exhibiting higher friction at high loads, despite involving less than a third of the amount of dextran (on a monomer basis) in comparison to the loop-train-tail system. The coefficient of friction at high loads decreased with increasing dextran surface density in the loop-train-tail system, while the opposite was true for the polymer brush. The surface density required to forestall the pressure-induced transition to high friction was also significantly higher for the loop-train-tail system than for the brush system. These results illustrate the influence of brush regularity on resistance to collapse under applied load, but also its role in exacerbating friction forces.

Introduction

Surfaces bearing densely packed, end-grafted neutral or charged polymer chains in good solvents are extraordinarily resistant to the intrusion of foreign bodies, leading to their characteristic low-friction and non-fouling behavior.[1,2] Particularly interesting are brushes composed of hydrophilic biocompatible polymers, such as poly(ethylene glycol), which have been the subject of many investigations as non-fouling surfaces, aqueous lubricants, and so-called "stealth coatings" against undesired immune-system response.[3-6] These characteristics, observable over a wide range of chain chemistries and architectures, originate from the steric hindrance presented by the chains and their associated solvent molecules, as well as the osmotic pressure induced by the strong interactions of the chains with the solvent.[7] The architecture of polymer-brush-mediated aqueous tribosystems also bears a striking similarity to that of naturally occurring lubricious systems, including the glycocalyx on the inner walls of capillaries,[8] the surface of articular cartilage,[9] and slippery surfaces such as the eye and tongue.[10] Such natural systems typically consist of oligosaccharide-bearing surfaces in aqueous environments. A characteristic feature of oligo- and polysaccharide chains is the presence of hydroxyl groups, which can directly engage in hydrogen bonding with adjacent chains, in contrast to polymers such as poly(ethylene glycol), for which water intercalation is necessary to bridge between chains. Hydroxyl groups also facilitate selective functionalization of the chains to produce films with complex architectures by the addition of reactive groups, branching, or crosslinking. Synthetic polysaccharide brushes and thin films have been produced by various means, including covalent grafting to silica surfaces,[11] Langmuir-Blodgett films of block copolymers,[12] and electrostatic adsorption of graft copolymers.[13,14]

In order to better understand the roles of the film architecture and inter-chain hydrogen bonding in polysaccharide films, we compared the friction behaviour of two different dextran-based architectures. Dextran is a naturally occurring hydrophilic polysaccharide consisting of D-glucose monomers connected by a-1,6 glycosidic linkages, which confer a relatively high degree of flexibility and prevent the formation of stable crystalline structures. PLL-*g*-dextran consists of dextran chains end-grafted to some of the pendant lysine groups of poly(L-lysine).[13-16] The unreacted lysine groups are positively charged under aqueous conditions at physiological pH, and thus facilitate spontaneous adsorption of the PLL-*g*-dextran molecule from solution onto negatively charged surfaces, such as silicon dioxide, with sufficient chain density to force the hydrophilic dextran chains into a brush conformation, as shown in Figure 1. PLL-*g*-dextran brushes in water are highly

RSC Advances Accepted Manuscript

lubricious against a hard counterface at low loads, but the friction increases sharply above a critical load.[17,18] When the counterface consists of a dextran brush, lower friction is obtained at low loads, the critical load is higher, and friction is higher above the critical load.

A high-coverage, PLL-*g*-dextran-functionalized surface probably represents the highest dextran brush density achievable via grafting-to means, with adsorption eventually limited by steric hindrance of the adsorbed brush, and largely independent of the number of unreacted lysine "feet" or the dextran or PLL chain lengths.[13,14,19] Since there is no readily available route to achieve higher dextran surface densities in a uniform brush, an alternative method of attaching dextran to the surface has been pursued. In the present study, substrates were coated with the adhesion promoter, poly(allylamine)-*graft*-perfluorophenylazide (PAAm-*g*-PFPA), an azide-bearing graft copolymer, and chain-density gradients of dextran chains were subsequently fabricated, being attached at random points to form a complex loop-train-tail structure, as shown in Figure 1. The influence of the chain density and applied load on the friction coefficient of the resulting film was investigated, and the results contrasted to the behaviour of PLL-*g*-dextran brushes.

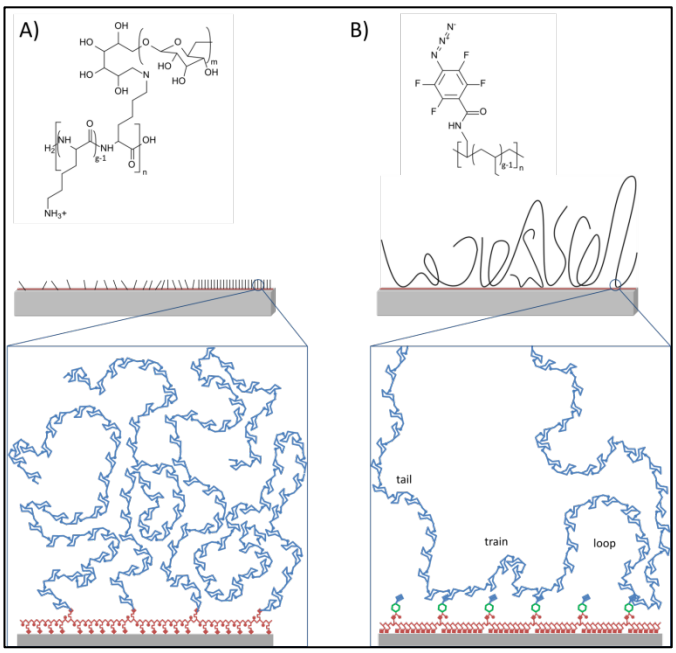

Figure 1 Chemical structures of poly(L-lysine)-*graft*-dextran (PLL-*g*-dextran) (A) and poly(allylamine)-*graft*-perfluorophenylazide-dextran (PAAm-*g*-PFPA-dextran) (B), and the corresponding expected polymer architectures, when attached to silicon oxide substrates.

Materials and methods

Synthesis of poly(allylamine)-*graft*-perfluorophenylazide (PAAm-*g*-PFPA)

Poly(allylamine)-*graft*-perfluorophenylazide (PAAm-*g*-PFPA) was synthesized as previously described.[20] Briefly, poly(allylamine hydrochloride) (6.33 mg, 6.8×10^{-6} mol monomer, 15 kDa, Sigma) and excess potassium carbonate (15.82 mg, 1.1×10^{-4} mol, Merck) were dissolved in 1.3 mL of water (Milli-Q Gradient A10, Millipore SA, Molsheim, France), and a solution of N-hydroxysuccinimide-perfluorophenylazide (NHS-PFPA, 5.62 mg, 1.7×10^{-5} mol, SuSoS AG, Dübendorf, Switzerland) in 1.3 mL of ethanol (Merck) was slowly added. The resulting solution was stirred overnight and then diluted to 100 mL with a 3:2 (v/v) ethanol/water mixture, yielding a polymer concentration of 0.1 g/L. All solutions were kept in the dark to avoid activation of the azide groups. The grafting ratio, defined as the number of allylamine monomers divided by the number of grafted PFPA monomers, is observed to be 8 or 9.[20]

Substrate preparation and dextran attachment

Bare 2 cm x 2 cm silicon wafers were cleaned by sonication twice for five minutes in toluene, then twice for five minutes in 2-propanol, after which they were exposed to O2 plasma for two minutes (Plasma Cleaner/Sterilizer, PDC-32G instrument, Harrick, Ossining, NY, USA). The surface SiO2 layer was characterized by ellipsometry, as described below, with none of the wafers exhibiting more than 0.1 nm variation, after which the wafers were immediately immersed in a 0.1 g/L solution of PAAm-*g*-PFPA. After thirty minutes of immersion, the substrates were rinsed and then sonicated for 5 minutes in a 3:2 (v/v) ethanol/water mixture, then rinsed with ultrapure water and dried with nitrogen. The PAAm-*g*-PFPA thickness was then measured by ellipsometry (described below).

Following this, the wafers were placed on a spin coater, covered in a solution of 25 g/L dextran (dextran T200, 2 MDa, Pharmacosmos A/S, Denmark) in water, and then spun at 4000 rpm for 40 s, then 5000 rpm for 10 s. The wafers were allowed to dry for 15 minutes, then exposed to UV light (Philips TUV 11W, peak wavelength 254 nm) at a distance of 10 cm. Dextran gradients were produced by varying the UV exposure time (from 3.5 s to 240 s) along the wafer using a moving shutter,[21] programmed to evenly space the desired exposure durations in discrete steps along the wafer. Following the UV exposure, the wafers were immersed overnight in ultrapure water to remove excess non-attached or physisorbed polymer, then rinsed with water, dried with nitrogen, measured by ellipsometry, and then stored in a dark prior to friction measurements.

The success of this method in achieving the desired system has previously been confirmed with XPS, ToF-SIMS and VASE.[20,21] Subsequent UV illumination in ambient air or in air with 100% relative humidity, with the aim of activating any remaining azides, was found to influence neither the thickness nor the friction measurements, within experimental error. Samples produced using lower molecular weights of dextran were found to yield significantly lower chain densities in addition to lower overall layer thickness, presumably due to less efficient covalent attachment related to the conformation of the spin-coated chains; the same trend has also been observed for other polymers.[20] Since the goal of the study was to obtain thicker, denser dextran brush-like films, these lower molecular weight films were not pursued further.

Characterization by Variable-Angle Spectroscopic Ellipsometry

Thickness measurements of the substrate SiO_2 layer, the adsorbed PAAm-*g*-PFPA layer, and the attached dextran film were performed in air using an M-2000 variable angle

RSC Advances Accepted Manuscript

This journal is © The Royal Society of Chemistry 2012

spectroscopic ellipsometer (VASE, J.A. Woollam Co., Inc., Lincoln, NE, USA) at a reflection angle of 70° and over the wavelength range of 370-994 nm. The spectra were analysed using WVASE32 software, using a multilayer model of Si/SiO_2 and top films with the optical properties of a Cauchy layer,[22] as detailed in the Supporting Information. The surface density of each layer can be calculated from the measured thickness and the bulk density of PAAm-*g*-PFPA and dextran.[20] Ellipsometric measurements on the gradient in water were also made using a liquid cell, and the results evaluated using the Bruggeman effective-medium approximation,[23] whereby the top layer was treated as a mixture of dextran (n=1.51) and water (n=1.333), and the layer thickness and dextran fraction were both fitted. The multilayer models for the dry and wet systems are shown in the Supporting Information.

Atomic Force Microscopy Measurements

The AFM experiments were conducted in contact mode by means of a MFP-3D AFM (Asylum Research, Santa Barbara, CA, USA) with gold-coated rectangular Si cantilevers (CSC12B, nominal normal spring constant 1.75 N/m, Mikromasch, Tallinn, Estonia), chosen to match the loading range of interest, while maintaining sensitivity and minimizing errors due to in-plane bending.[24] A borosilicate colloidal sphere (Kromasil, Eka Chemicals AB, Bohus, Sweden; radius ~8 μm) was glued to the end of the cantilever with UV-curable epoxy. (Norland Optical Adhesive #63, Norland, Cranbury, NJ, USA) The entire assembly was then irradiated with UV light for 30 minutes and left for a full day prior to use, to further strengthen the adhesion between the colloidal sphere and the cantilever.

Friction measurements were obtained by scanning the probe perpendicularly to the major axis of the cantilever and recording the TMR (Trace Minus Retrace in mV) value. The TMR value is directly proportional to the friction force and minimizes the contributions to the lateral force from non-friction sources.[25] The gradient was characterized by measuring points in a random order, in order to minimize possible effects arising from gradual drift. All scans were 1 μm in length with velocities of 1 μm/sec. The dependence of lateral force on scanning distance was investigated and it was shown that for scans longer than 100 nm, the lateral force remained constant. All friction measurements were performed in ultrapure water.

The normal and lateral cantilever spring constants were calibrated prior to sphere attachment from the power spectral density of the thermal noise fluctuations[26] and by the method of Sader and coworkers.[27] The lateral force measurements of the rectangular cantilevers were calibrated using the test-probe method described by Carpick and coworkers,[28] yielding absolute values for both the lateral force and the local coefficient of friction (the ratio of lateral to normal force). The test-probe calibration method itself includes correcting factors for differences in cantilever dimensions, colloidal sphere size, normal and lateral spring constant of the cantilever, and spot intensity between the experimental and reference setups. All experiments were measured within a gradient in a single run with the same tip and cantilever. Additionally, all the rectangular cantilevers used for the calibration and measurement were produced in a single batch from the same wafer, so that any errors stemming from non-ideal behaviour of the cantilevers or unaccounted factors, such as variations in the reflectivity of the cantilever top coatings, would be consistent across all measurements.

Following nanotribological measurements with an uncoated borosilicate colloidal probe, the entire tip-cantilever assembly was gently lifted off the gradient surface and immediately exposed to a 0.02 mg/mL PLL-*g*-dextran (synthesized from previous work)[13,14] solution to form a dextran brush layer on the probe surface. After 30 minutes, the assembly was thoroughly rinsed with water and placed back into contact with the same gradient substrate to resume the friction experiments.

Results and discussion

Gradient fabrication

The VASE dry thickness of the PAAm-*g*-PFPA layer was 1.7 + 0.1 nm, and the additional dry thickness of the attached dextran film reached 6 nm at the dense end of the gradient, corresponding to a density of 36 dextran monomers per nm^2, or 343 nm^2 per 2MDa dextran chain. The kinetics of the UV-activated attachment of dextran to the substrate are seen to approximate a logarithmic curve until reaching saturation after about one minute, as shown in Figure 2. The aqueous VASE measurements indicate a relatively constant (water + dextran) film thickness of 124 + 5.4 nm, independent of the UV irradiation time, while the fraction of dextran within the film increased with increasing UV irradiation, as shown in Figure 3. Films produced with the shorter irradiation times could not be reproducibly measured in the wet state due to weak signal.

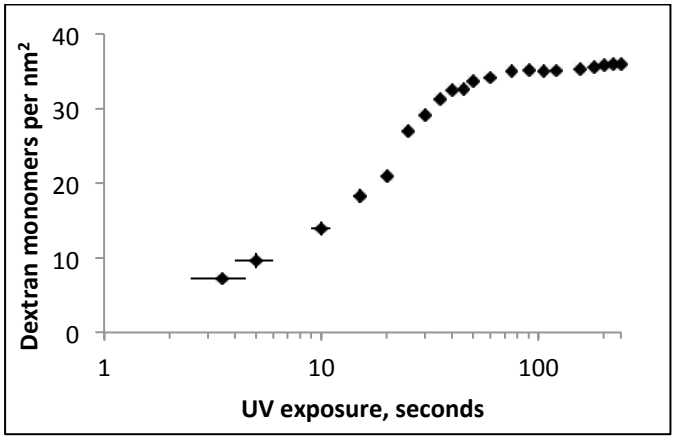

Figure 2 Surface density of dextran in PAAm-*g*-PFPA-dextran films, calculated from VASE thickness measurements, plotted against UV exposure time.

Comparing the surface densities of dextran and PAAm-*g*-PFPA calculated from these VASE measurements at the densest end of the gradient, and taking the experimental grafting ratio of 9 allylamines to each PFPA, we obtain 542 PFPA units per 2 MDa dextran chain, or 56.9 dextran monomers per PFPA unit, with 1.58 PFPA units per nm^2. What fraction of these PFPA units is actually bound to a dextran is unknown. However, since the kinetics are roughly logarithmic until the saturation point, and neither the wet height nor the friction changes appreciably upon further UV irradiation, we conjecture that relatively few PFPA units are bound to the dextran chains, and attempt to estimate the number of attachment points from the measured values.

Assuming that the chain is attached to the PFPA layer at equidistant points along the chain, and that these can be treated as single attachments (therefore neglecting trains), then the film

RSC Advances Accepted Manuscript

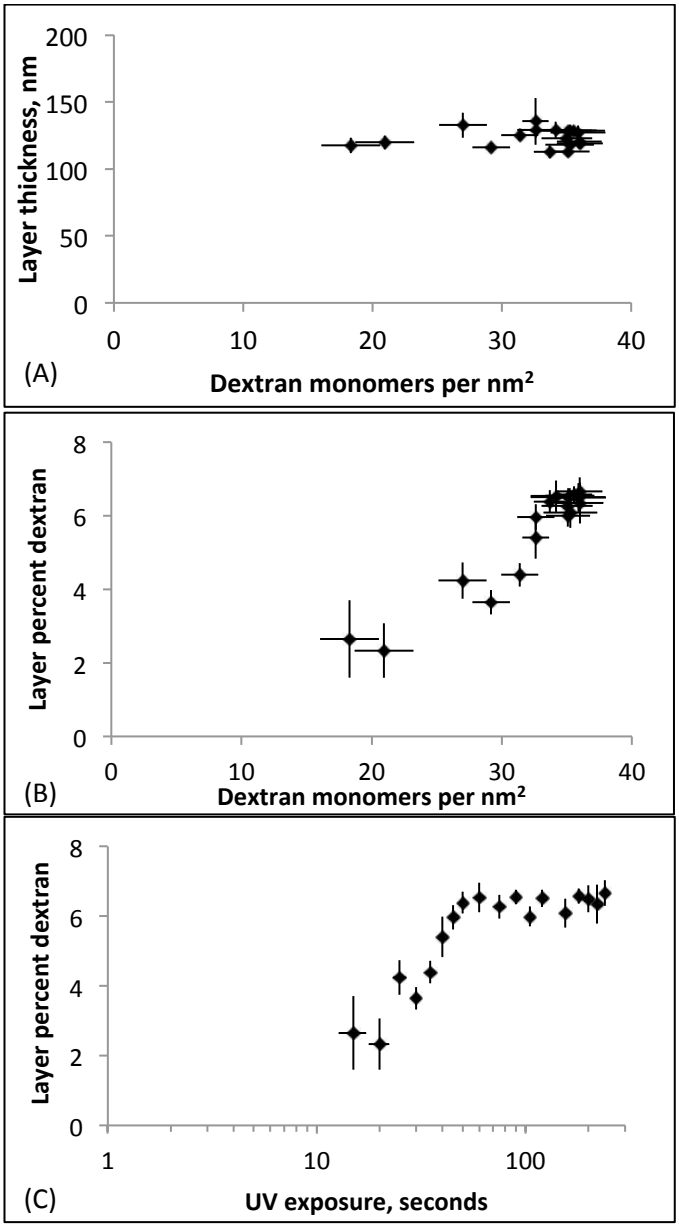

Figure 3 Thickness (A) and mass fraction (B) of the dextran/water layer associated with the PFPA-coated substrate, measured by VASE in a water-filled liquid cell and calculated using the Bruggeman mean-field approximation, plotted against the dextran surface density. Mass fraction is also plotted against UV exposure time (C) for comparison of the kinetics with those in Figure 2.

can be treated as a "brush" consisting of two end tails and a number of loops in the middle, with the spacing between points such that the tail and loop lengths are equal, as shown in the Supporting Information. For example, if a 2 MDa chain is bound at two points, then that chain can be treated as two 500 kDa tails and a 1 MDa loop, which approximates to four equally spaced 500 kDa end-attached chains. If these effective 500 kDa chains are swollen in liquid to their bulk hydrodynamic radius,[29] the theoretical film thickness can be calculated from the measured dextran surface density, and compared to the measured value. Replacing the single-point attachments with short trains would not significantly influence the result. The best agreement with the measured wet thickness of the film was achieved when the 2 MDa chain was bound at three points, yielding two 333 kDa tails and two 666 kDa loops, which if equated to an effective brush of six 333 kDa chains would have a theoretical film thickness of 125.5 nm at the densest end of the gradient. While there are numerous sources of error in this calculation, it supports the hypothesis that each chain is bound by only a few PFPA units. A uniform 333 kDa brush of the measured density would have an $L/2R_g$ value of 0.21, taking R_g to be 19 nm.[30]

Friction measurements

The friction coefficient of the PAAm-*g*-PFPA-dextran films is highly load dependent, with all but the sparsest films exhibiting a low-friction regime at low loads. A transition to a high-friction regime occurs above a critical normal load, as shown in Figure 4. This behavior is similar to that observed in PLL-g-dextran brushes,[17,18] and Figures 5 and 6 show the results from that study alongside the results of the PAAm-*g*-PFPA-dextran findings for comparison. Figure 5 shows the friction coefficient in the low- and high-load regimes plotted against the dextran monomer density, while Figure 6 shows the critical normal load at which the friction increases, also plotted against the dextran monomer density. All measurements were performed against a bare borosilicate sphere as well as a PLL-*g*-dextran-coated sphere under aqueous conditions.

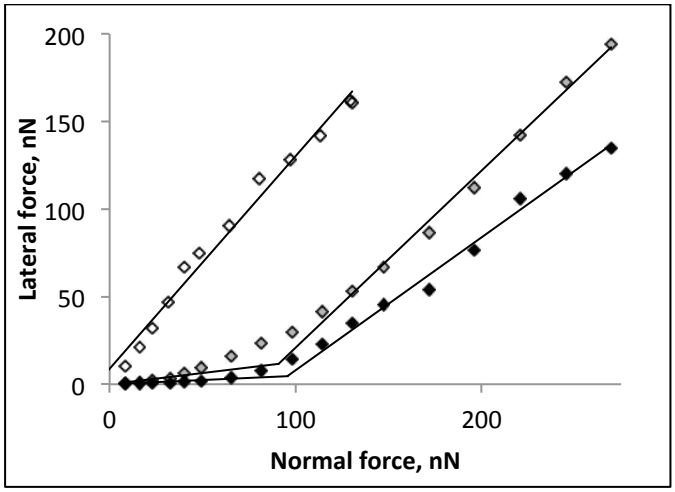

Figure 4 Typical friction vs. load curves of a colloidal probe sliding on a PFPA-*g*-dextran-coated wafer exposed to UV for 5 seconds (yielding a coverage of 9 dextran monomers/nm^2, white), 20 seconds (24 monomers/nm^2, grey), and 120 seconds (35 monomers/nm^2, black). Fits of the linear parts of each series, excluding the non-linear intermediate points, are extrapolated to their intersecting point, the x-coordinate thereof representing the transition load.

The "low-load" and "high-load" regimes in Figure 5 correspond to the distinct friction regimes shown in Figure 4: the "low-load" regime for each measurement represents the range from the lowest load until the transition load, calculated from the intercepts of the respective slopes shown in Figure 4 (if such a low-friction regime exists). The "high-load" regime extends from the transition load to the maximum load tested. The transition loads are dependent on brush density, as shown in Figure 6. In order to avoid the ambiguity of the nonlinear slope near the transition region, the intersection of linear fits of the

RSC Advances Accepted Manuscript

This journal is © The Royal Society of Chemistry 2012

low- and high-load regimes is taken as the transition load. Note that only the x-coordinate of the transition point, the applied load, is considered. This method of calculating friction coefficients and transition loads has been shown previously.[17] It should be noted that even in the "low load" regime, a simplified Hertzian analysis shows that the maximum pressures are on the order of ~50 MPa—far higher than typical contact pressures observed in natural joints.[17]

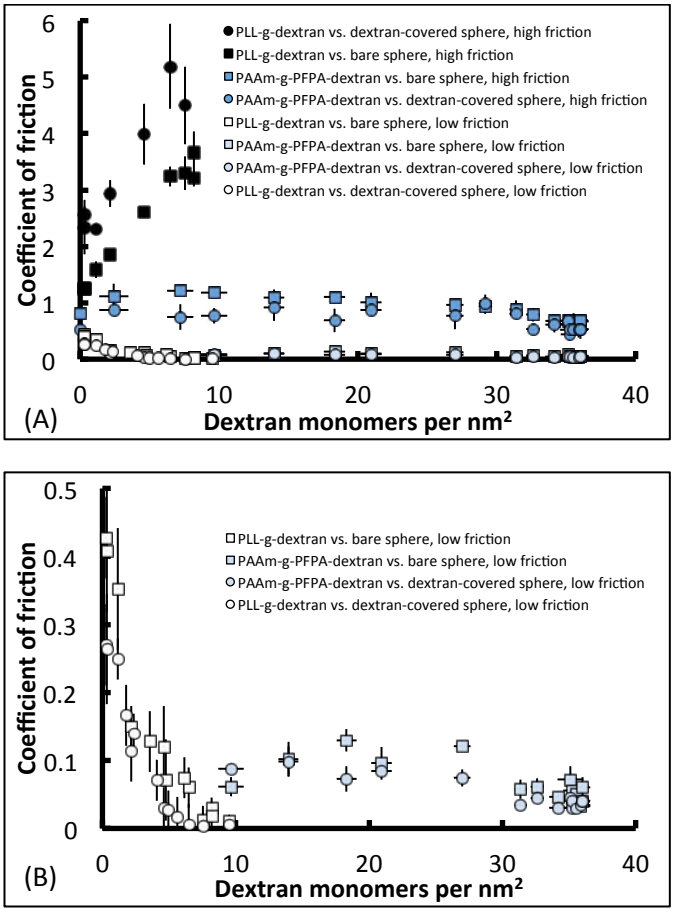

Figure 5 Coefficient of friction of PLL-*g*-dextran[17] (black and white) and PAAm-*g*-PFPA-dextran (blue) plotted against surface density of dextran monomers in both low and high load regimes (A) and just the low load regimes (B, zoomed in from A). The squares represent a bare borosilicate sphere at low load (white or light blue) and high load (black or dark blue). The circles represent a PLL-*g*-dextran coated borosilicate sphere at low load (white or light blue) and high load (black or dark blue).

The PAAm-*g*-PFPA-dextran system, consisting of a more disordered loop-train-tail architecture, showed a higher friction coefficient at low loads compared to the brush formed by PLL-*g*-dextran, despite the greater wet film thickness and much higher surface monomer density. However, the disordered system showed a lower friction coefficient at high loads compared to the brush system, with the coefficient of friction decreasing as the dextran density increased, while the opposite was true for the brush. The transition from low to high friction regimes also occurred at much higher dextran surface monomer concentrations in the disordered case than for the brush, indicating that the disordered system is less able to support high loads. The lower dextran coverages in the disordered case were unable to achieve brush-like low friction values under any load, and therefore only showed the high-friction regime, as shown in Figures 4 and 6. Finally, the impact of dextran-coating the borosilicate sphere is opposite in the high-friction regime, with the dextran coating exacerbating friction in the brush case while reducing it in the disordered case.

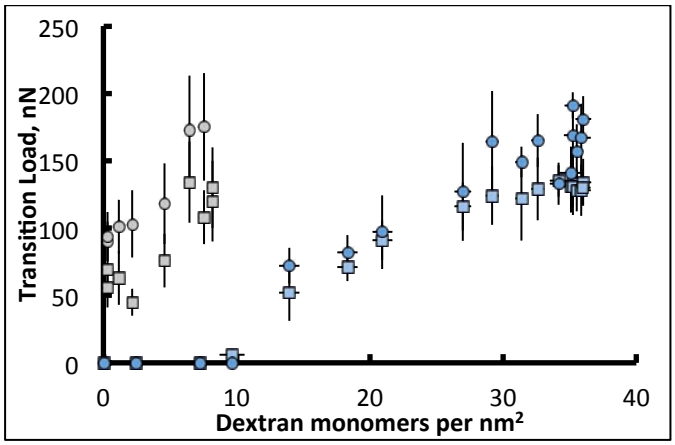

Figure 6 Critical load associated with the transition from low to high friction regimes of PLL-*g*-dextran[17] (grey) and PAAm-*g*-PFPA-dextran (blue) plotted against surface density of dextran monomers. The squares represent a bare borosilicate sphere, while the circles represent a PLL-*g*-dextran coated borosilicate sphere.

The significance of the brush conformation has been demonstrated previously by collapsing brushes with minimal changes to the solvent,[31] which dramatically changes the mechanical properties of the film. In the absence of significant hydrodynamic forces, longer, more disordered systems will significantly interpenetrate and interact under even low loads. Brush interpenetration increases friction even when inter-chain interactions from opposing substrates, such as tangling or hydrogen bonding, are neglected.[32] Tangling is also known to increase friction coefficient between polymer brushes,[33-36] although tangling is not possible for the 5 kDa dextran chains, since they are too short and stiff. However, the interpenetration of chains under high loads, with the subsequent formation of inter-chain hydrogen bonds, nevertheless creates high friction between the surfaces.[17] The impact of interpenetration, entanglement and hydrogen bonding together, as in the case of the dextran loop-train-tail system, is more complex. While hydrogen bonding between chains on the same substrate may inhibit entanglement with chains of the counterface at low loads, the application of higher loads and lateral forces does ultimately yield increased friction, which is controlled by inter-chain association as well as tangling.[37]

The combination of increased chain entanglement and hydrogen bonding between the counterfaces can explain the differences between the disordered, thicker dextran system and the brush system. The friction coefficient of the brush is lower at low loads, due to its density and the lack of tip interpenetration, thanks to the inter-chain hydrogen bonding holding the chain ends in place. As the load increases, the ordered brush system is more capable of resisting this

RSC Advances Accepted Manuscript

interpenetration than the disordered system, which more rapidly becomes enmeshed with the counterface. However, the ordering and hydrogen bonding show the opposite effect once interpenetration is achieved, with interactions between opposing surfaces of ordered chains creating much more resistance than is the case for the longer, disordered conformation, where the chains are freer to rearrange themselves.

While these findings are significant in the field of brush and thin-film design, they are most pertinent to the case of more complex architectures, in which gels and brushes may be combined in various ways to achieve tailored properties. For example, it has been shown that short polymer brushes on top of gels reduce their friction, while long polymer brushes increase it,[38] a phenomenon that seems likely to be related to the differences outlined here.

Conclusions

The lubricating properties of a dextran surface-density gradient, attached at random intervals to the surface by means of an intermediate azide-bearing monolayer, were investigated by means of colloidal-probe lateral force microscopy. The results were contrasted with previous work involving density gradients of end-attached dextran (a polymer brush density gradient). Both systems showed highly load-dependent friction, with the randomly attached dextran chains exhibiting less extreme differences than the polymer-brush case. For the randomly attached system, significantly higher surface concentrations of dextran were necessary to reach the same critical load (marking the transition from low to high friction regimes). This suggests that the polymer-brush architecture significantly enhanced the load-bearing properties of the dextran film. Increasing the density of the disordered dextran film reduced the friction coefficient at high loads, while the opposite was true for the polymer brush. These findings demonstrate that the brush architecture is critical in resisting collapse under applied load, but is susceptible to inter-chain interactions between the surfaces, which increase friction once the load has exceeded a critical threshold. This highlights the tradeoff involved in designing film architectures to maximize layer thickness and lubricity under extreme loads or to aim for an ideal brush with ultra-low friction at low and moderate loads. Future work on heterogeneous architectures may allow tailored films that exhibit the appropriate mixture of properties, depending on the expected loading of the film.

Acknowledgements

The authors are grateful for financial support by the Swiss National Science Foundation.

Notes and references

[a] Laboratory for Surface Science and Technology, Department of Materials, ETH Zurich, Vladimir-Prelog-Weg 5, CH-8093 Zurich, Switzerland.

[b] Swiss Federal Institute for Materials Science and Technology, Empa, Ueberlandstrasse 129, CH-8600 Duebendorf, Switzerland. * Correspondence should be addressed to R.C. (rowena.crockett@empa.ch).

Electronic Supplementary Information (ESI) available: XXXXXXX

1 W. H. Briscoe, S. Titmuss, F. Tiberg, R. K. Thomas, D. J. McGillivray and J. Klein, *Nature*, 2006, **444**, 191.
2 D. Dowson, *History of Tribology*, Professional Engineering Publishing, London, 1998.
3 G. L. Kenausis, J. Vörös, D. L. Elbert, N. Huang, R. Hofer, L. Ruiz-Taylor, M. Textor, J. A. Hubbell and N. D. Spencer, *J. Phys. Chem. B*, 2000 **104**, 3298.
4 N.-P. Huang, R. Michel, J. Voros, M. Textor, R. Hofer, A. Rossi, D. L. Elbert, J. A. Hubbell and N. D. Spencer, *Langmuir*, 2001, **17**, 489.
5 S. Lee and N. D. Spencer, in *Superlubricity*, Elsevier Science B.V., Amsterdam, 2007, Ch. 21.
6 S. Lee, M. Müller, M. Ratoi-Salagean, J. Vörös, S. Pasche, S. M. de Paul, H. A. Spikes, M. Textor and N. D. Spencer, *Tribol. Lett*., 2003, **15**, 231.
7 S. T. Milner, *Science,* 1991, **251**, 905.
8 D. Dowson, *Faraday Discuss.,* 2012, **156**, 9.
9 B. Zappone, M. Ruths, G. W. Greene, G. D. Jay and J. N. Israelachvili, *Biophys. J.*, 2007, **92**, 1693.
10 S. Lee and N. D. Spencer, *Science,* 2008, **319**, 575.
11 S. Martwiset, A. E. Koh and W. Chen, *Langmuir*, 2006, **22**, 8192.
12 W.T.E Bosker, K. Patzsch, M. A. C. Stuart and W. Norde, *Soft Matter*, 2007, **3**, 754.
13 C. Perrino, S. Lee, S. W. Choi, A. Maruyama and N. D. Spencer, *Langmuir*, 2008, **24**, 8850.
14 C. Perrino, S. Lee and N. D. Spencer, *Tribol. Lett.*, 2009, **33**, 83.
15 A. Ferdous, H. Watanabe, T. Akaike and A. Maruyama, *Nucl. Acids Res.*, 1998, **26**, 3949.
16 A. Maruyama, H. Watanabe, A. Ferdous, M. Katoh, T. Ishihara and T. Akaike, *Bioconjug. Chem.*, 1998, **9**, 292.
17 K. J. Rosenberg, T. Goren, R. Crockett and N. D. Spencer, *ACS Appl. Mater. Interfaces*, 2011, **3**, 3020.
18 T. Goren, R. Crockett and N. D., Spencer, *CHIMIA*, 2012, **66**, 192.
19 S. Pasche, S. M. De Paul, J. Vörös, N. D. Spencer and M. Textor, *Langmuir*, 2003, **19**, 9216.
20 Â. Serrano, O. Sterner, S. Mieszkin, S. Zürcher, S. Tosatti, M. E. Callow, J. A. Callow and N. D. Spencer, *Adv. Func. Mater.*, 2013, **23**, 5706.
21 O. Sterner, Â. Serrano, S. Mieszkin, S. Zürcher, S. Tosatti, M. E. Callow, J. A. Callow and N. D. Spencer, *Langmuir*, 2013, **29**, 13031.
22 E. Palik, *Handbook of optical constants of solids*, New York Academic, Orlando, 1985.
23 D. A. G. Bruggeman, *Ann. Phys. Leipzig*, 1935, **24**, 636.
24 J. E. Sader and C. P. Green, *Rev. Sci. Instrum.*, 2004, **75**, 878.
25 E. Meyer, *Prog. Surf. Sci.,* 1992, **41**, 3.
26 S. M. Cook, T. E. Schaffer, K. M. Chynoweth, M. Wigton, R. W. Simmonds and K. M. Lang, *Nanotechnology*, 2006, **17**, 2135.
27 J. E. Sader, J. W. M. Chon and P. Mulvaney, *Rev. Sci. Instrum.*, 1999, **70**, 3967.
28 R. J. Cannara, M. Eglin and R. W. Carpick, *Rev. Sci. Instrum.,* 2006, **77**, 053701.
29 K. A. Granath, *J. Coll. Sci.*, 1958, **13**, 308.
30 J. K. Armstrong, R. B. Wenby, H. J. Meiselman and T. C. Fisher, *Biophys. J.*, 2004, **87**, 4259.
31 O. Azzaroni, S. Moya, T. Farhan, A. A. Brown and W. T. S. Huck, *Macromolecules*, 2005, **38**, 10192
32 A. Nomura, K. Okayasu, K. Ohno, T. Fukuda and Y. Tsujii, *Macromolecules*, 2011, **44**, 5013.
33 J. Klein, in *Fundamentals of Tribology and Bridging the Gap Between the Macro- and Micro/Nanoscales*, Kluwer Academic Pub., Dordrecht, 2001, p. 177.

RSC Advances Accepted Manuscript

 This journal is © The Royal Society of Chemistry 2012

34 U. Raviv, S. Giasson, N. Kampf, J.-F. Gohy, R. Jérôme and J. Klein, *Nature,* 2003, **425**, 163.
35 B. Liberelle and S. Giasson, *Langmuir,* 2008, **24**, 1550.
36 F. Goujon, P. Malfreyt and D. J. Tildesley, *Macromolecules*,2009, **42**, 4310.
37 D. M. Loveless, N. I. Abu-Lail, M. Kaholek, S. Zauscher and S. L. Craig, *Angew. Chem.,* 2006, **118**, 7976.
38 Y. Ohsedo, R. Takashina, J. P. Gong and Y. Osada, *Langmuir*, 2004, **20**, 6549.

RSC Advances Accepted Manuscript

Table of contents

Impact of chain morphology on the lubricity of surface-grafted polysaccharides

The impact of brush-like structure and disorder on the lubricating ability of dextran chains at low and high loads has been investigated using AFM.

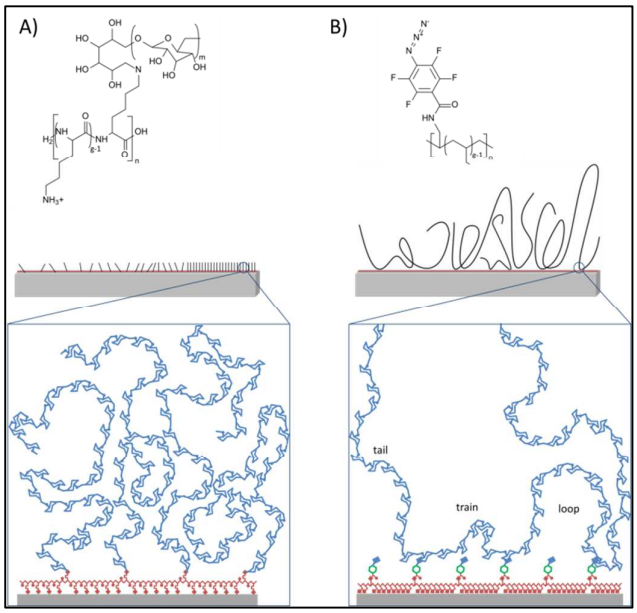

RSC Advances Accepted Manuscript